Chapter 3

Spatial Relationships of MR Imaging and Positron Emission Tomography with Phenotype, Genotype and Tumor Stem Cell Generation in Glioblastoma Multiforme

Davide Schiffer, Consuelo Valentini, Antonio Melcarne, Marta Mellai, Elena Prodi, Giovanna Carrara, Tetyana Denysenko, Carola Junemann, Cristina Casalone, Cristiano Corona, Valentina Caldera, Laura Annovazzi, Angela Piazzi, Paola Cassoni, Rebecca Senetta, Piercarlo Fania and Angelina Cistaro

Additional information is available at the end of the chapter

http://dx.doi.org/10.5772/58391

1. Introduction

Glioblastoma multiforme (GBM), the most malignant and frequent glioma, is a heterogeneous tumor in which areas of different histological aspect, aggressiveness, genetic expression and regressive events coexist so that one region of the tumor is not representative of the entire neoplasia. The consequences of the heterogeneity reflect on the diagnostics, prognostics and therapies. As a matter of fact, unguided surgical biopsies can lead to sampling error and to undergrade the tumor up to 30% of cases [1]. From the surgical, but also prognostic and therapeutic point of view, it is of great importance to know in advance the composition of the tumor and the biological significance of the different imaging aspects. Neuro-imaging is the only and fundamental source of information for the neurosurgeon and it has progressed today from the simple anatomic recognition of the tumor to that of functional and metabolic significance of its different regions, contributing greatly to a better approach to tumor surgery, prognosis and therapy. The detection of highly malignant regions and the definition of the tumor extent are crucial before the operation, when they are the main concern of neurosurgeons.

GBM is composed, as it is universally known, of three zones: central necrosis, proliferation and infiltration zones (Figures 1,2). Proliferation region is characterized by high indices of cell

density, proliferation, mitoses, vessel density or angiogenesis and circumscribed necroses. In the spectrum of the many aspects of the tumor, with the term disruption one indicates the passage from the uniform and quiescent appearance of an astrocytoma to the rupture of the structure, forms and dimensions of GBM (Figure 3A). Circumscribed necroses and angiogenesis are the absolute features of GBM and their occurrence is needed for its recognition, because they are direct signs of malignancy (Figures 3B,4A-C). Angiogenesis in gliomas represents the intervened transformation, whereas it depends on the imbalance between the high proliferation potential of tumor cells and the low reproduction capacity of endothelial cells [2]. When the diagnosis has to be carried out on small tumor samples, as for example in stereotactic biopsies, the diagnosis cannot be of certainty. When close to central necrosis, circumscribed necroses merge with it. Infiltration zone represents the invasion into the brain of tumor cells that acquire a particular phenotypic and molecular signature. It is not uniform along the tumor borders and often it is so mild that it is hardly detectable, also histologically. Frequently, it is discovered in histological sections only after counting the cells and this happens either when it affects the white matter or the cortex, where tumor cells must be distinguished from normal cells. In the latter, perineuronal satellitosis may be of help. Isolated tumor cells (ITCs) in the normal nervous tissue make the problem of the tumor delimitation very hard. They cannot be detected, of course, in the samples removed during intervention, but only in the study of the brain at autopsy and they can be found very far from the tumor borders; the classic example is the passage of normally looking corpus callosum by ITCs [3,4]. Regressive events are frequent and include haemorrhages, large necroses, vascular thrombosis, *etc* and they contribute to the so-called disruption of the tissue.

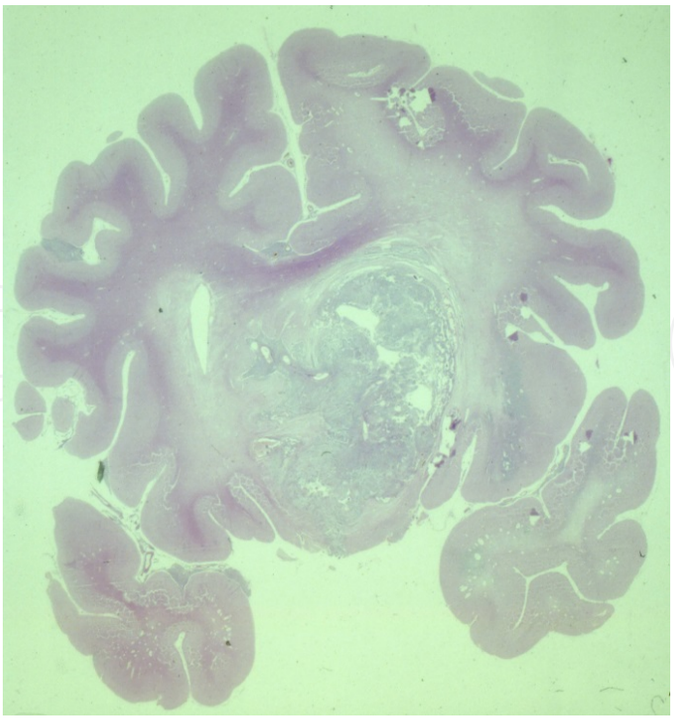

Figure 1. Coronal section of a brain with GBM. The borders of the tumor show different nervous structures. H&E.

http://dx.doi.org/10.5772/58391

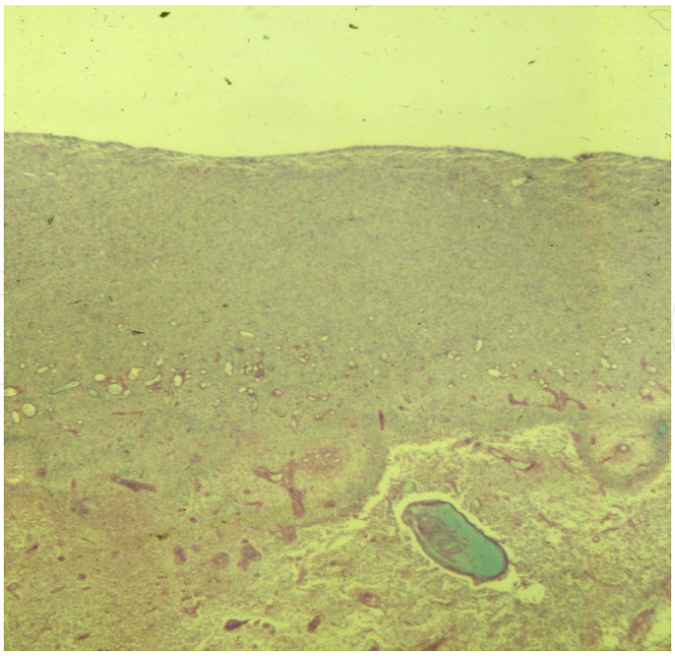

Figure 2. Three zones can be recognized: central necrosis, proliferation, and infiltration zone. H&E, 25x.

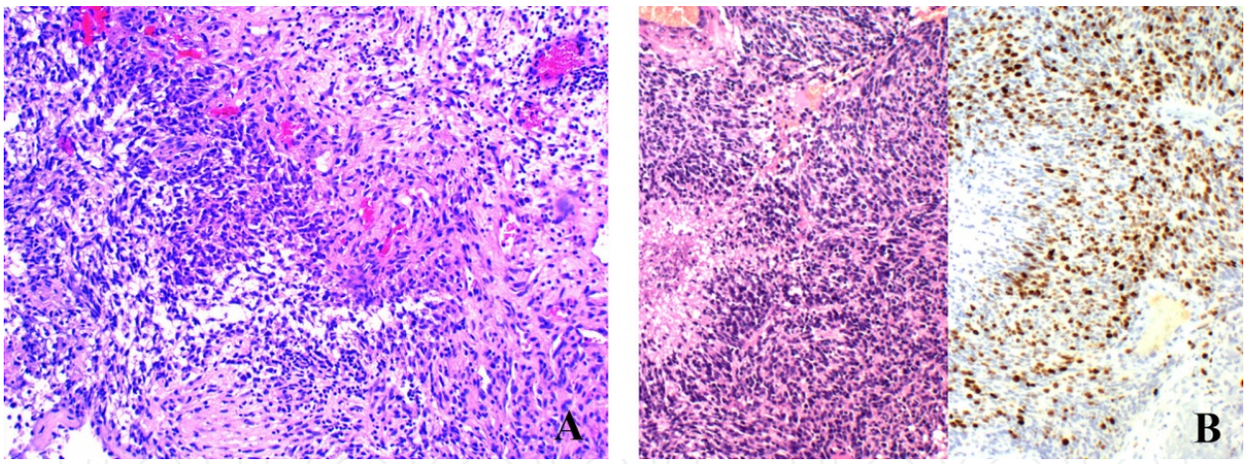

Figure 3. A – Area of disrupture with high cell density, vessels of different size and edema dissociation of the tissue; B – Circumscribed necrosis with pseudo-palisading in an area with high cell density (H&E, 100x) and area with a high Ki-67/MIB.1 proliferation index (DAB, 100x).

Beside the classic T1 and T2 imaging of GBM, supplied by the anatomy based magnetic resonance (MR), physiology-based MR imaging methods, namely diffusion-weighted imaging (DWI), perfusion-weighted imaging (PWI) and proton MR spectroscopy imaging (MRSI), together with the positron emission tomography (PET), which is highly correlated with the degree of malignancy [5,6], improved the tumor characterization. Today, the advancement of the knowledge in molecular biology and cell biology, associated with new surgical procedures, radiation techniques and therapeutic possibilities ask the neuro-imaging to answer three main questions: the identification *in vivo* of the tumor sites with the highest malignancy grade, the

extension of tumor invasion and the sites where the capacity of the tumor to reproduce, to recur and to resist therapies resides, *i.e.* where the so-called glioblastoma stem cells (GSCs) are located.

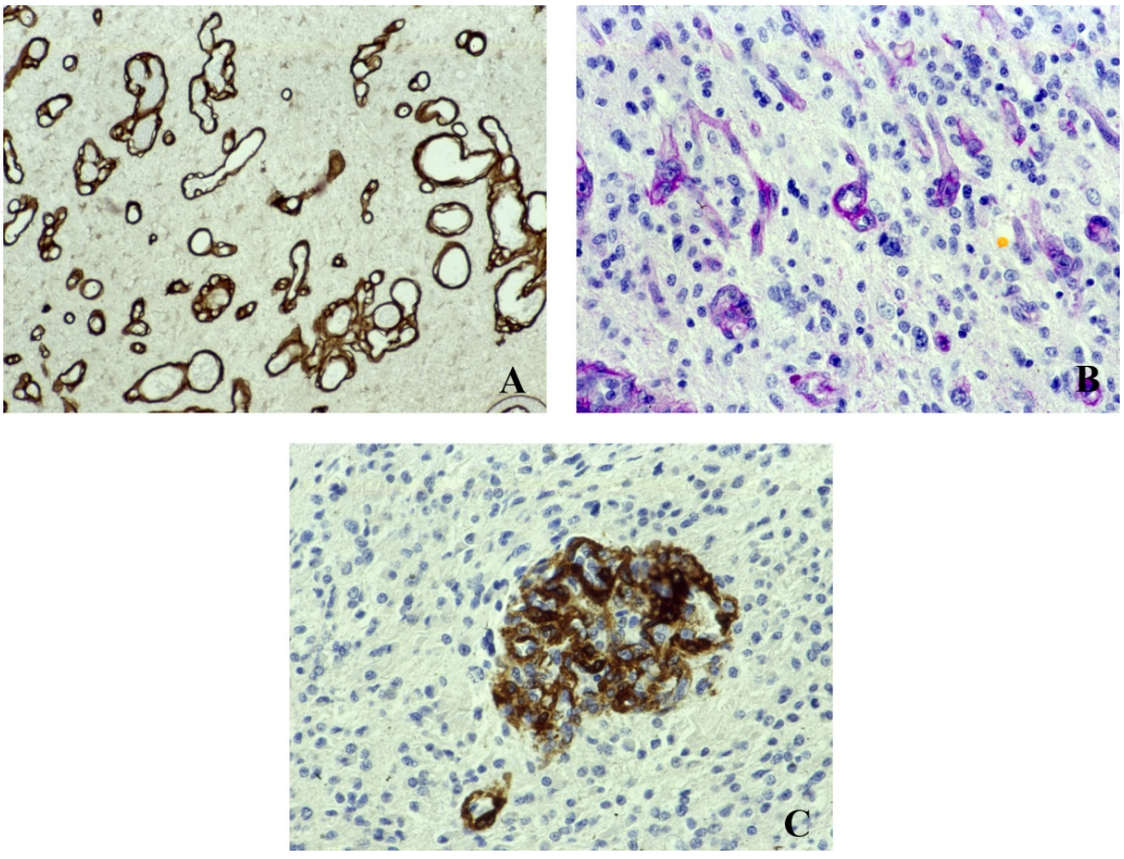

Figure 4. A – High vessel density. Laminin, DAB, 100x; B – Neoformed vessels and endothelial buds. PAS, 200x; C – Glomeruloid structure. α-sm-actin, DAB, 200x.

2. Physiology based MRI and PET

DWI rationale is to quantify the brownian movement of water protons within tissues that depends on the complex interaction between the intracellular and extracellular compartments, but also on cell density, cell membrane permeability and tissue structure. Water diffusivity within the extracellular compartment is inversely related to cell size and cell number. The greater the volume of the intracellular space and also the higher the cell density, the lower is the water diffusivity in the extracellular space, resulting in a low apparent diffusion coefficient (ADC), a measure of water diffusion. Diffusivity within tumors is heterogeneous due to different tumor components, being reduced in areas with high cellular density and increased in necrotic regions. Restricted ADC values in a tumor can also be related to ischemic changes, haemorragic or calcific components.

Although several reports have shown that glioma grade inversely correlates with intra-tumor minimum ADC [7], reflecting the presence of areas with high cell density in high grade tumors [8,9], the clinical significance of ADC measurement is limited as a consequence of the tissue heterogeneity within a tumor and because of substantial overlap in ADC values among different grades of glioma [10,11]. The range of ADC values within a given glioma, therefore, can vary markedly [11] and there is no final confirmation that minimum ADC always correlates with cell density.

PWI is used to measure vascularization and perfusion of brain lesions. Different PWI techniques are available, namely dynamic susceptibility contrast (DSC) and dynamic contrast-enhanced (DCE), widely used in the clinical setting. DSC perfusion measures T2-weighted signal-intensity loss occurring dynamically over a bolus injection of contrast medium, from which relative cerebral blood volume (rCBV), a marker of tumor angiogenesis, can be computed. DCE is a T1-weighted sequence that measures vascular permeability in tumors during a bolus injection of contrast medium; rCBV values are then calculated from DCE data. rCBV values have shown good correlation with the World Health Organization (WHO) tumor grading [12,13]; exceptions are represented by low-grade glial neoplasms with oligodendroglial features and grade I pilocytic astrocytoma, that may have markedly elevated rCBV (Figure 5).

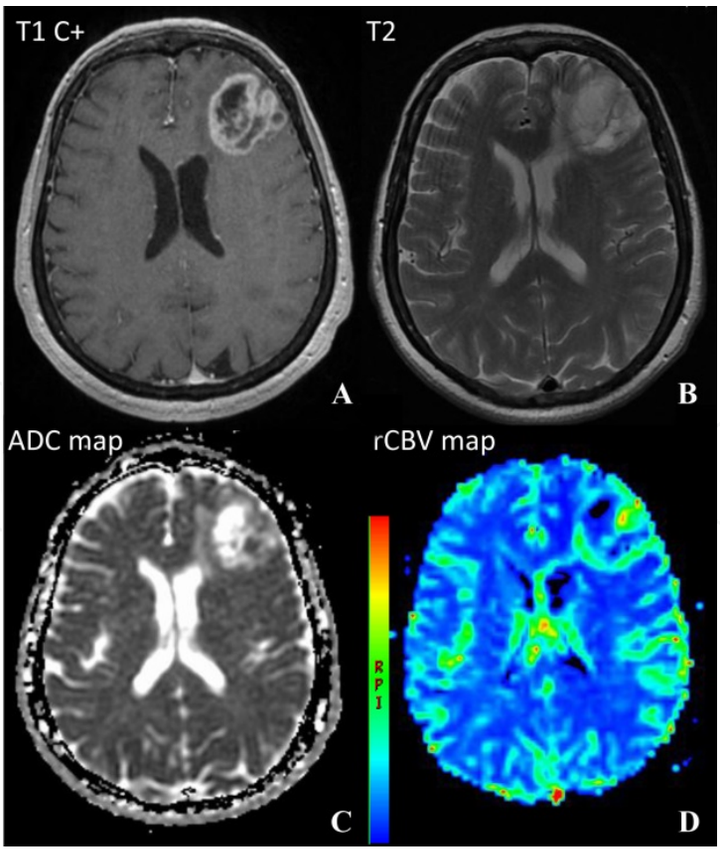

Figure 5. A –T1C MRI; B – T2 MRI; C – Diffusion MRI; D – Perfusion MRI.

Arterial spin-labeling (ASL) is a more recent perfusion technique that uses water of the blood entering the brain as an endogenous tracer to evaluate perfusion. ASL is emerging as an alternative to gadolinium based techniques in the evaluation of tumor perfusion.

MRSI is another advanced technique that provides metabolic information of the brain tissue. The predominant metabolites are choline (Cho), N-acetylaspartate (NAA), creatine (Cr), glutamate and glutamine (Glx), myo-inositol (MI) and lactate/lipids (LL). The Cho peak contains contributions from several different choline-containing compounds, which are involved in membrane synthesis and degradation; NAA is marker of neuronal integrity; Cr is a marker of cellular energetics; MI is considered a glial cell marker; LL are markers of tissue breakdown and anaerobic glycolysis. Glx is a complex peak from glutamate (Glu), glutamine (Gln) and gamma-aminobutyric acid (GABA). Glu is an important excitatory neurotransmitter and it also plays a role in the redox cycle. In brain tumors, as malignancy increases, NAA signal decreases, as a consequence of loss, dysfunction or displacement of normal neurons, while Cho levels increase as a consequence of rapid cell membrane turnover. Malignant tumors also have reduced Cr due to high metabolic activity that depletes the energy stores; this is associated to anaerobic glycolysis leading to the appearance of lactate. Necrotic portions of tumor show the presence of lipid peaks. Elevated concentration of Gln can be found in high grade tumors.

Metabolite concentrations are usually expressed as ratios (*i.e.* Cho/Cr, Cho/NAA, NAA/Cr) rather than as absolute concentrations.

Such spectra can be obtained using single voxel or multi-voxel 2D or 3D technique. Multi-voxel spectroscopy is the best to detect infiltration of malignant cells beyond the enhancing margins of tumors [14,15] (Figures 6,7).

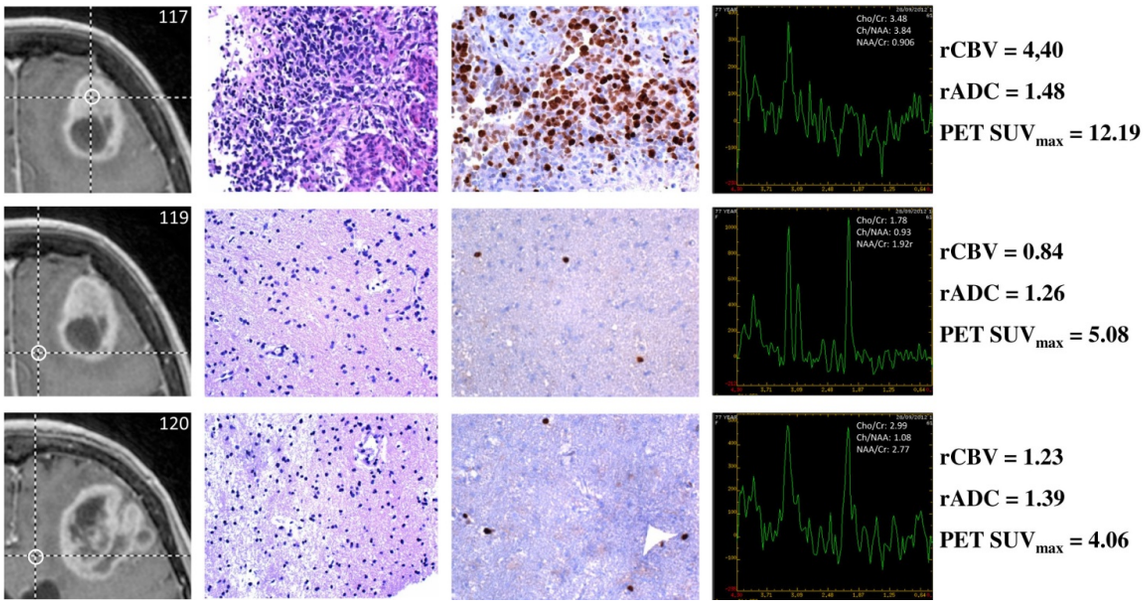

Figure 6. Case CTO3. Correlation among histopathology, Ki-67/MIB.1 proliferation marker, MRSI, physiologic MRI and PET values. Column 1 – ROIs on T1C MRI; Column 2 – Histopathology of a hyper-proliferating area and two areas differently infiltrated. H&E, 200x; Column 3 – Ki-67/MIB.1 proliferation index, DAB, 200x; Column 4 – MRSI values; Column 5 – PET values.

http://dx.doi.org/10.5772/58391

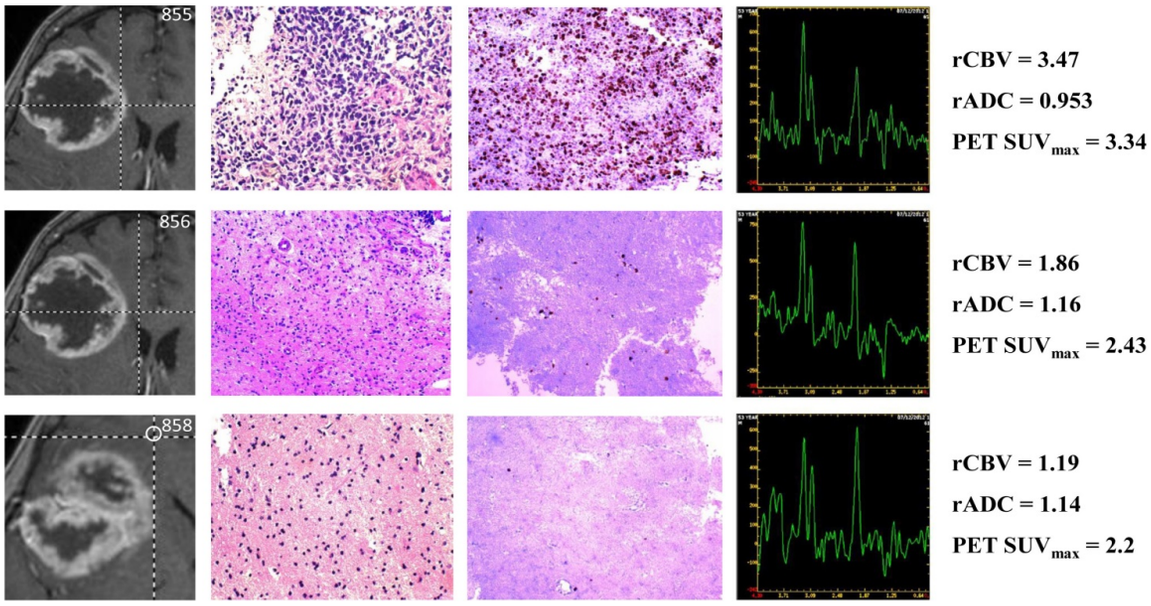

Figure 7. Case CTO5. Correlation among histopathology, Ki-67/MIB.1 proliferation marker, MRSI, physiologic MRI and PET values. Column 1 – ROIs on T1C MRI; Column 2 – Histopathology of a hyper-proliferating area and two areas differently infiltrated. H&E, 200x; Column 3 – Ki-67/MIB.1 proliferation index, DAB, 200x; Column 4 – MRSI values; Column 5 – PET values.

Diffusion tensor imaging (DTI) is an advanced MRI technique that describes the movement of water molecules using two metrics, mean diffusivity (MD) and fractional anisotropy (FA), that represent the magnitude and directionality of water diffusion, respectively. FA technique measures the preferential direction of proton movement and varies among values between 0 (isotropic diffusion, *i.e.* random diffusion such as in brain gray matter) and 1 (anisotropic diffusion, such as in brain white matter where proton diffusion is constrained along myelin fibres). MD technique gives information on the whole diffusivity in the brain; the reduction of nervous fibres results in an increased MD because of a higher degree of freedom of movement of water molecules. The degree of anisotropy depends on many factors, such as fibre density and diameter, myelin sheath integrity and the intercellular space characteristics. In the presence of a structural alteration of the nervous fibre tract, the anisotropic value reduces.

Anisotropy is reduced in cerebral lesions due to the loss of structural organisation. The measurement of FA allows prediction of histological characteristics such as cellularity, vascularity, or fibre structure. This technique is useful to differentiate normal white matter from edematous brain tissue and occult white matter invasion around the enhancing portion of the tumor.

DTI may help to determine the white matter fibre displacement by tumor. This technique, in combination with functional neuro-imaging methods, permits to map the individual anatomo-functional connectivity and represents a useful tool for surgical planning [16-18].

PET is currently the most powerful method of molecular imaging, as it has been emphasized in a recent review [19] (Figure 8). Depending on the radiotracer, various molecular processes can be visualized by PET, most of them relating to an increased cell proliferation within

gliomas. Radiolabeled 2-[18F]fluoro-2-deoxy-D-glucose ([18F]FDG), methyl-[11C]-L-methionine ([11C]MET) and 3-deoxy-3-[18F]fluoro-L-thymidine ([18F]FLT) are taken up by proliferating gliomas depending on their tumor grade as the consequence of an increased activity of membrane transporters for glucose ([18F]FDG), amino acids ([11C]MET), and nucleosides ([18F]FLT) as well as increased expression of cellular hexokinase ([18F]FDG) and thymidine kinase ([18F]FLT) genes, which specifically phosphorylate [18F]FDG and [18F]FLT, respectively [20]. Imaging of brain tumors with [18F]FDG was the first oncologic application of PET. [18F]FDG is actively transported across the blood-brain barrier (BBB) into the brain where it is phosphorylated and trapped into cells. Since 1982 [5,21], PET with [18F]FDG has been accepted and widely used in the grading of brain tumors; its uptake is generally high in high-grade tumors and it has a good prognostic value, because increased intra-tumoral glucose consumption correlates with tumor grade [22], biological aggressiveness and survival of patients in both primary and recurrent gliomas. Pathology and survival can be predicted by [18F]FDG-PET in gliomas [6]. In addition, a tumor-to-white matter ratio and tumor-to-gray matter ratio were found to increase the sensitivity of the grading evaluation [22]. Since intratumor heterogeneity of brain tumors is not adequately revealed in conventional MRI, because evaluation of the contrast enhancing lesion can either under-or overestimate the presence of active tumor, MRSI and PET are requested to gain additional information on metabolic and molecular tumor markers. In a tumor, the grading can be heterogenous with low-and high-grade areas, as it happens frequently in GBM. This may affect the choice of the site for stereotactic biopsy, which must direct towards tumor sites with the highest tumor grade. Therefore, suitable targets for biopsy will have positive contrast enhancement on T1-weighted MRI, a high choline-peak on MRSI and hypermetabolism on [18F]FDG-PET, the uptake of which is much higher in high-grade component of tumors. As a matter of fact, the [18F]FDG-PET improved the diagnostic yield of stereotactic biopsies by detecting metabolically active areas of tumor [23].

However, [18F]FDG-PET can have some diagnostic limitations, because of the high rate of physiologic glucose metabolism in normal brain tissue. In the brain cortex it is particularly high [24,25], so when a hypermetabolic lesion is close to the cortex or the subcortical white matter, the distinction of the tumor from the normal tissue may be difficult [22]. Moreover, it must be taken into account that [18F]FDG accumulation can be non-specific, because it is also observed in inflammatory or granulation tissues [26]. A later PET image acquisition [27] and a co-registration of PET images with MR images greatly improves the performance of [18F]FDG-PET [28]. Technologic advances have allowed to merge PET and MR images, combining the high resolution of MR imaging with the low-resolution functional capability of PET [23], defined as a reduction of intracellular oxygen pressure (pO2), because of decreased supply and of increased demand for oxygen. It predicts poor treatment response of malignant tumors. Two different forms of tumor hypoxia are recognized. Diffusion-limited chronic hypoxia may develop as a result of increased intercapillary distances, and acute hypoxia can result from occlusion of large tumor vessels [29]. Both forms of hypoxia have several implications for the further evolution of tumors (induction of signaling cascades that promote angiogenesis, growth, and cell migration) [30]. Tumor hypoxia may also lead to necrosis, which is mandatory to establish the diagnosis of GBM. The **([18F]Fluoromisonidazole) ([18F]FMI-**

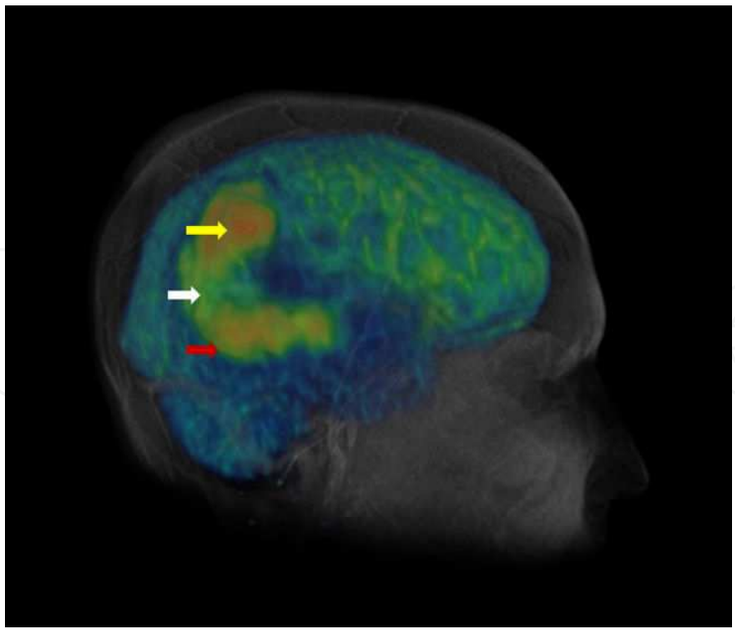

Figure 8. Female 22-year-old affected by GBM. Maximum intensity projection (MIP) fusion PET/3D spgr MRI image showing extensive lesion involving the right parietal-temporal lobe with heterogeneous increased [18F]FDG uptake, due to the lesion heterogeneity: high-grade component presenting elevated [18F]FDG activity with standardized uptake value $(SUV)_{max=}17$ (yellow arrow), intermediate-grade component presenting $SUV_{max}=12$ (white arrow), low-grade component $SUV_{max}=4$ (red arrow).

SO) is a nitroimidazole derivative, a PET agent used for hypoxia detection. [18F]FMISO-PET can image tumor hypoxia by increased [18F]FMISO tumor uptake, because [18F]FMISO metabolites are trapped exclusively in hypoxic cells. It accumulates in both hypo-and hyper-perfused tumor regions, suggesting that hypoxia in GBM may develop irrespective of the magnitude of perfusion [31].

3. Biological significance of MRI variables in GBM

Basically, three conditions can be detected with anatomy-based MRI: iso-hypo-intensity in TC1 (tumor, edema), hyper-intensity in TC2 (edema) and contrast enhancement (malignancy). The contrast enhancing regions (CERs) of untreated GBM correspond to the most histologically malignant areas of the tumor with architectural disruption, high cell density, proliferation, vessel density and angiogenesis with circumscribed necroses. Many other properties are revealed by physiology-based MRI. In CERs, in comparison with non-enhancing regions (NERs), physiologic MRI variables show higher values of rT1C, relative fast spin echo (rFSE), rCBV, relative peak height (rPH) and relative recovery factor (rRF), whereas rADC, relative fractional anisotropy (rFA) and fluid attenuated inversion recovery (rFLAIR) do not differ from NERs. All these observations have been shown and confirmed in recent studies of many cases of GBM planning pre-operatively tissue sampling sites and marking them on the anatomic images used by the surgical navigation work station. A comparison between MRI variables and histology of the samples corresponding to the MRI regions of interest (ROIs) in

CERs and NERs has been made [32,33]. A correlation of histopathologic features and DWI and DSC variables prevailed in enhancing areas and rCBV and Cho/NAA index (CNI) above and rADC below a certain value could indicate the occurrence of tumor cells. Neoangiogenesis could be recognized and distinguished from simple endothelial hyperplasia, even though the permeability of the region is limited. Interestingly, also T2 rFSE and rFLAIR hyperintensity areas could show histopathologic features of malignancy. On the whole, it was demonstrated by gene microarray that the genetic expression patterns between CERs and NERs were different, with genes associated with mitosis, angiogenesis and apoptosis clustered in CER surgical samples [32].

The values of MRSI variables such as Cho/Cr and Cho/NAA showed a parallel variation as those of DWI and PWI. In spite of the possibility of a misregistration between biopsy sites and MRI uploaded to the neuronavigation device if a brain shift occurs, GBM histologic features could be usefully identified by physiology-based MRI [33].

Using the same technique, *i.e.* combining physiology-based MRI, MRSI and [18F]FDG-PET imaging with neuronavigation work station in a series of gliomas, mainly GBMs, we observed that the values of rCBV, ADC, Cho/Cr, CNI were useful for recognizing tumor areas and their phenotypic variations, as for both the number of cells and vascular pathologic structures (Figures 6,7). A possible source of error was the mismatch between the MRI registration and the sampling by the navigator, so that a dissociation between the variable values of the ROIs and histopathology occurred. For example, a ROI on central necrosis could erroneously correspond to a high rCBV value and histologically to the occurrence of tumor tissue in the sample. However, this was a rare event and it did not prevent from recognizing the biological significance of the imaging values contained in the ROIs, also by extrapolation among all the samples.

Malignant gliomas are hypermetabolic in comparison with normal brain. The glycolytic metabolism is increased as well as protein and membrane synthesis to maintain the rapidly dividing tumor cells. MRSI in spite of an intra-or inter-subject variability can identify the tumor. There are two patterns clearly distinct: one is that corresponding to the ROIs on necrotic regions and the other that on the enhancing ring. In the first one, two patterns have been in turn described: "necrosis" and "cystic necrosis" with variable Ch and high LL peak and with no peaks and variable LL, respectively. The ROIs on the ring show a high Cho and Cho/NAA ratio, whereas very variable are those on regions around the ring [34]. In our series Cho, Cho/Cr and Cho/NAA values were constantly high in CERs in comparison with NERs.

Fusing MRI and [11C]MET-PET it was shown that the volume of the radio-compound uptake is greater than that of gadolinium enhancement on T1, even though smaller than T2 volume; it extends beyond in most cases [35,36] correlating with the proliferation markers [37,38], increased Cho/NAA and DTI abnormalities in the white matter [28,39]. However, there could be an underestimation of the tumor extension, because infiltrating cells do not proliferate [3,40].

The number of genetic alterations decreased from the most malignant areas of the tumor to the peripheral areas, correlating fairly well with the MRI variable values and indicating the

occurrence or not of tumor cells. In particular, Epidermal Growth Factor Receptor (EGFR) amplification, the occurrence of EGFRvIII and Tumor Protein p53 (TP53) mutations were more frequent in CERs than in NERs, corresponding to a malignant histology. The genetic variability in the different samples was interpreted as due to polyclonality and not only to a genetic heterogeneity supported by the occurrence in the same tumor of different non-tumor cells of various species. Polyclonality means cell complexity, formed by tumor cells that differ among themselves for a series of phenotypic and molecular characteristics of cell proliferation, invasion, *etc.* [41,42]. This observation can be a warning against the use of small tumor samples to characterize the genotype of the entire tumor. Heterogeneity has been explained either by the hierarchic model mechanism [43] or by the stochastic mechanism [44] of tumor development. The two models, however, cannot be mutually exclusive, because their cells should derive from a common ancestor [45]. As for EGFR amplification, the possibility that its variation could depend on an asymmetrical distribution during mitoses must be mentioned [46,47], even if it is already included in the clone formation. The neurosphere assay produces neurospheres (NS), characterized by stemness antigens (Figure 9A,C,E), and adherent cells (AC), characterized by differentiation antigens (Figure 9B,D,F).

However, their phenotype is not the same in the different tumor sites, differing for the quota of the two types of antigens. There must be a different capacity of the tumor areas to host or to generate GSCs and this is in line with the concept that a GSCs hierarchy exists for their potential [48-52]. GSCs have been interpreted as the top of a hierarchy of tumor cells for stemness and, therefore, for self-renewing, clonogenicity, *etc.* They occur in tumor niches and are under the control of microenviroments with their intrinsic and extrinsic signaling [53,54]. The niches can be perivascular or perinecrotic [53] and for a series of observations and considerations they must develop in the most malignant sites of the tumor [51,55]. Stemness and differentiation are the opposite poles of a spectrum in which a hierarchy exists of GSCs as for their potential [48-52]. Going from areas of the highest malignancy, such those of CERs, to differentiated ones, the stem-cell potential decreases [55]. In this way the distribution of GCS in GBM could be explained. The NS and AC degree of differentiation or stemness, demonstrated by the relevant antigens, represents an interesting subject of study that has been pursued by us by confocal microscopy (unpublished data).

Confocal microscopy is an advanced technique of optical imaging used to obtain high resolution images [56,57]. In tissue and cells derived from GBM, it is possible to distinguish the emission signal of different markers and to perform study of both co-localization and quantification of the luminous signal related to the protein marker expression. The cellular heterogeneity is a hallmark of GBM. Using differentiation and stemness markers it is possible to identify hypothetical immature or dedifferentiated elements in the whole tumor cell population, as well as in NS or AC by the neurosphere assay. Confocal images of glioma cells by double immunofluorescence allow to distinguish the expression pattern of the markers above mentioned. Their expression levels, related to the intensity of the emitted signal, show variable Nestin and glial fibrillary acidic protein (GFAP) positivity, depending on the tumor site. The method has a paramount importance in the study of the spectrum from stemness to differentiation.

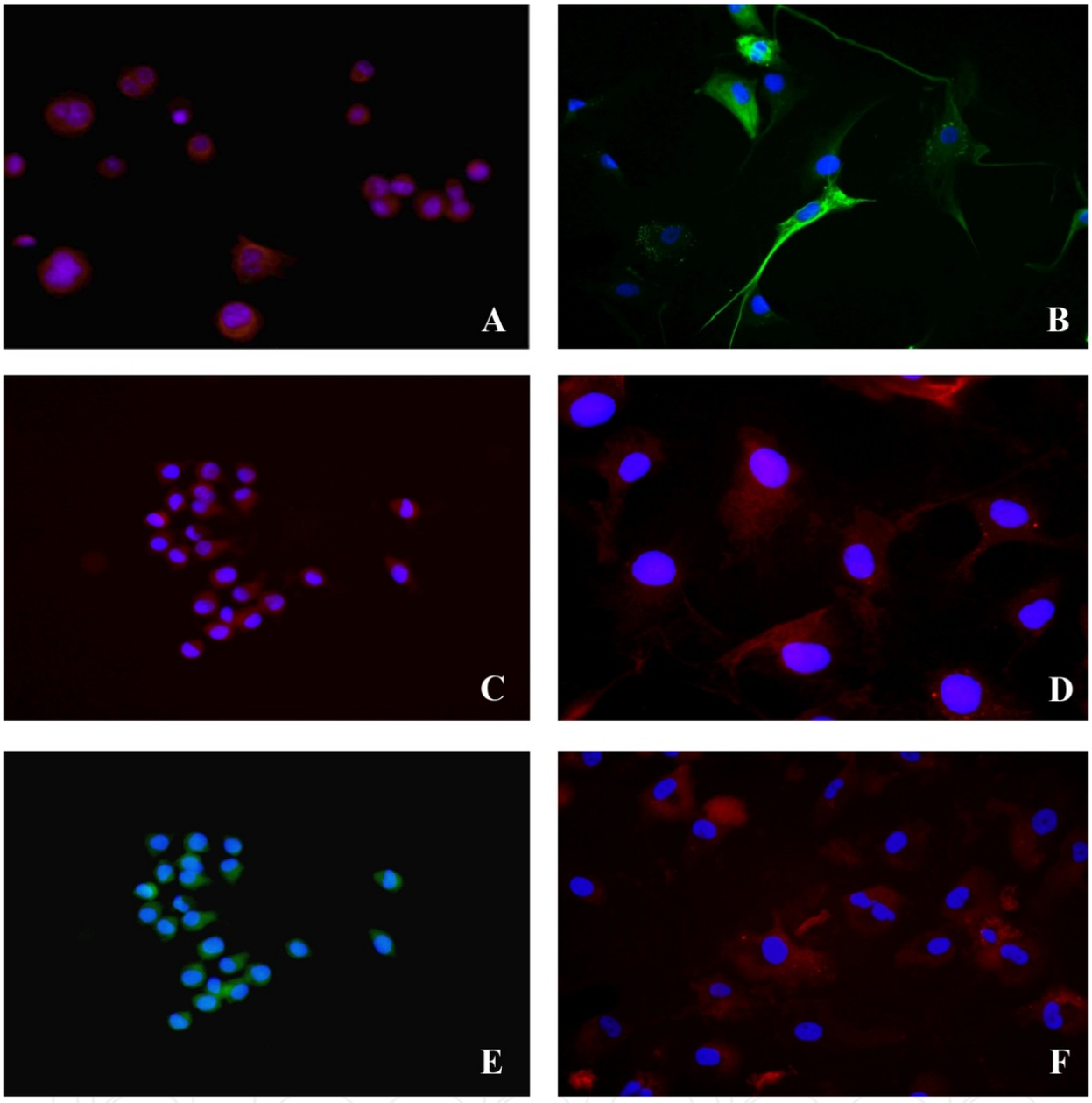

Figure 9. Immunofluorescence (IF) for stemness antigens in NS. A – Nestin, 200x; C – CD133, 200x; E – Musashi1, 200x. IF for differentiation antigens in AC. B – GFAP, 400x; D – GalC, 400x; F – β-III Tubulin, 400x. Nuclei are counterstained with DAPI.

4. The tissue around the tumor — Cell invasion and edema

Beside resistance to chemo-and radiotherapy, the failure of a local control of GBM by therapies is due to the modalities of tumor cell invasion into the brain. Surgical resection cannot prevent recurrence because of the occurrence of infiltrating cells; recurrence usually starts from the resection margin. The target volume for radiotherapy, therefore, conventionally includes the tissue within 2 cm from the MRI border of the tumor. This is for sparing normal nervous tissue from irradiation damage, but also for including in it infiltrating cells. Nevertheless, 80% of

http://dx.doi.org/10.5772/58391

tumors relapses within 2-cm margin around the enhanced region [58]; another adverse characteristic of infiltrating cells is that they do not proliferate [3,40], escaping thus detection and being less sensitive to treatments.

Tumor invasion is not uniform along its borders. It can be non-existent where the tumor sharply abuts against the normal nervous tissue (Figure 10A), as it may happen with the white matter, or it gradually progresses from the tumor outwards (Figure 10B). Typical is the invasion of the cortex from a tumor located in the white matter, even with the typical picture of perineuronal satellitosis (Figure 10C). The different invasion modalities have been codified [59] and a distinction between diffuse and local tumors has even been proposed [60], but it was not confirmed by the observation of substantially different outcomes.

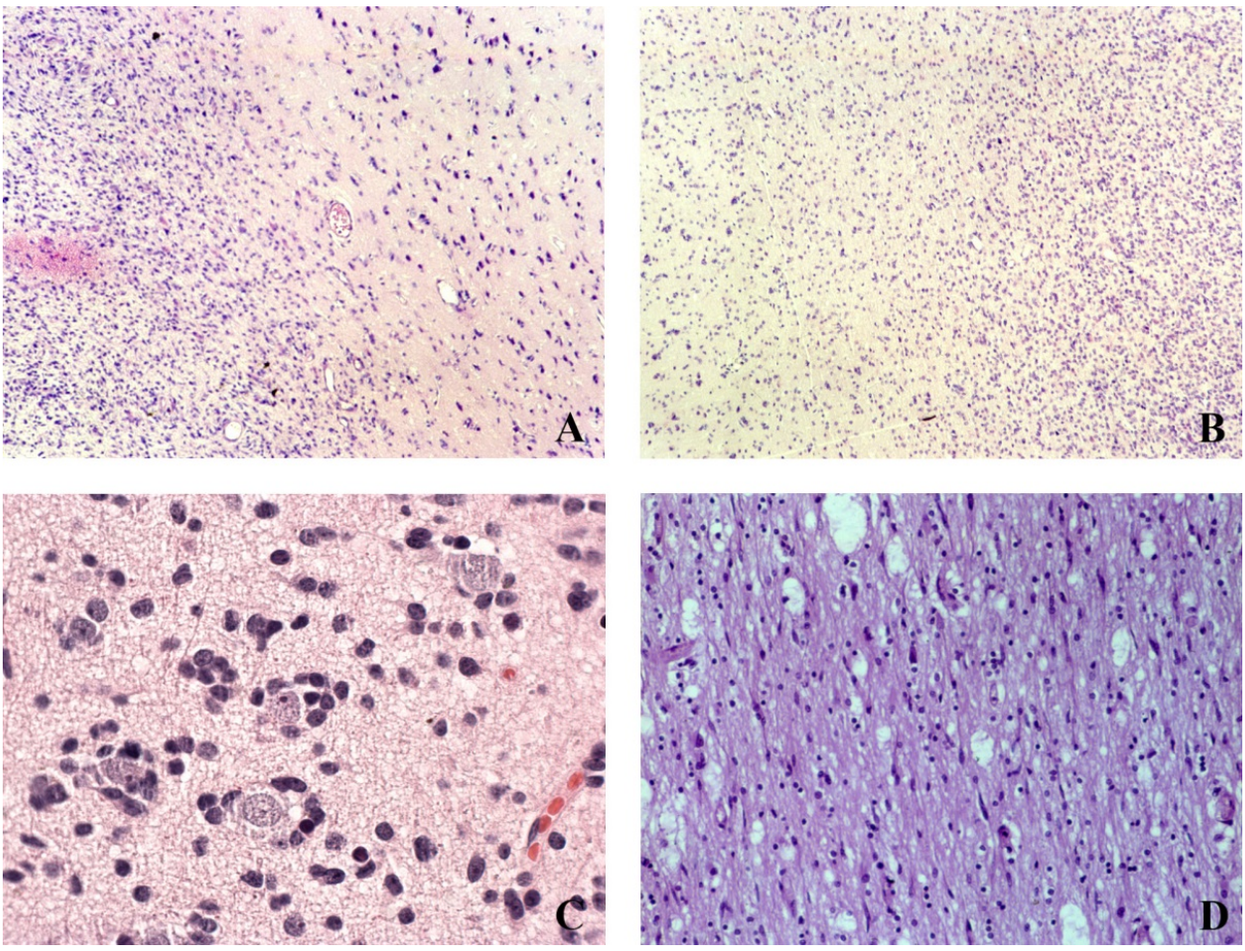

Figure 10. A – Sharp tumor border. Ki-67/MIB.1, DAB, 100x; B – Invasion gradient toward the cortex. H&E, 100x; C – Perineuronal satellitosis. H&E, 400x; D – Infiltration along corpus callosum. H&E, 200x.

Letting aside the mechanisms of tumor cell migration and invasion of which there is today a good knowledge [61-63], some information about neuropathologic findings on peritumor tissue are relevant. First of all, it has been demonstrated that patients with absence of tumor cells in the adjacent normal nervous tissue had better survival than those with tumor cells [64]. This is not in contrast with the observation that the removal of edematous peritumor tissue

does not improve the outcome of operated patients [65]. In this regard, residual cells after surgery have been interpretated as distinct from the cells found in routinely resected GBM tissue, as if they would represent a distinct, malignant GBM subentity [66]. A second important point is how to recognize invading cells. Beside nuclear abnormalities, there are only the counts of cells, as will be said. Nestin expression [67] and mainly Isocitrate Dehydrogenase isoforms 1 and 2 (IDH1/2) mutations [68] have been proposed, but it must be taken into account that primary GBM cells are IDH1/2 wild-type.

Cell infiltration, as it is usually seen in histological sections of tumor surgically removed, can be very mild and not easily recognizable without cell counts or decidedly evident (Figure 11A,B). Its aspects largely depend on the various modalities of GBM spreading and three main possibilities are recognized [69]: the distant spreading through corpus callosum (Figure 10D), septum pellucidum, *etc.*, the sub-pial invasion (Figure 11C) and the invasion of the cortex from the white matter where the tumor is located (Figures 11C). Also sub-arachnoidal seeding is frequent [70,71], sometimes as small clusters of tumor cells, visible at naked eyes from which tumor cells go down along penetrating vessels to invade the cortex (Figure 11D). It is very important to remark that invading cells do not proliferate, as it has been demonstrated *in vitro* [72,73] and *in vivo* [3,41,74]. Two other cell types can be found in peritumor tissue: macrophages/microglia and reactive astrocytes, both in edematous and non-edematous tissue. The former, independently of their influence on immunoregulation and tumor growth [61], are abundant in both tumor and peritumor tissue [75]; it has been calculated that up to one third of cells in glioma biopsies are represented by macrophages [75,76] (Figure 12B,C). Incidentally, a positive or negative relationship between microglia/macrophages and TICs is today discussed [77]. The same can be said for the possibility that microglia can be exploited in tumor therapy. It remains today "in its infancy" [78] as it happens for the possibility to inhibit microglia/macrophages in order to prevent their promotion of tumor progression [79].

Reactive astrocytes can be sometimes confused with tumor cells, mainly because their phenotype changes over time until complete maturation (Figure 12A). There are analogies between glial reaction and physiological maturation of astrocytes during embryogenesis. In initial phases, the fine processes originate directly from the cell soma and then from the thick and long processes [80]. Nestin and Vimentin would be the main intermediate filaments of immature astrocytes, whereas GFAP of the mature ones [81,82].

It is long debated whether infiltrated tissue can be recognized by MRI, not only when adjacent to tumor, but also at a distance. It has been observed, for example, that low-grade gliomas, which preferentially locate in the insula and the supplementary motor area, spread along distinct sub-cortical fasciculi [83]. Analyzing different peritumor areas with different MRI methods, it has been shown that FA and not apparent diffusion coefficient can be used to evaluate glioma cell invasion. An attempt to classify different peritumoral tissues by a voxel-wise analytical solution using serial diffusion MRI has been made [84].

Peritumoral reactive gliosis has a particular importance because of three main characteristics: reactive astrocytes divide by mitosis as tumor cells; they progressively lose Nestin and they increase GFAP expression as during development, and they may exert regionally a series of metabolic and molecular influences [61]. The most important point is that reactive astrocytes

http://dx.doi.org/10.5772/58391

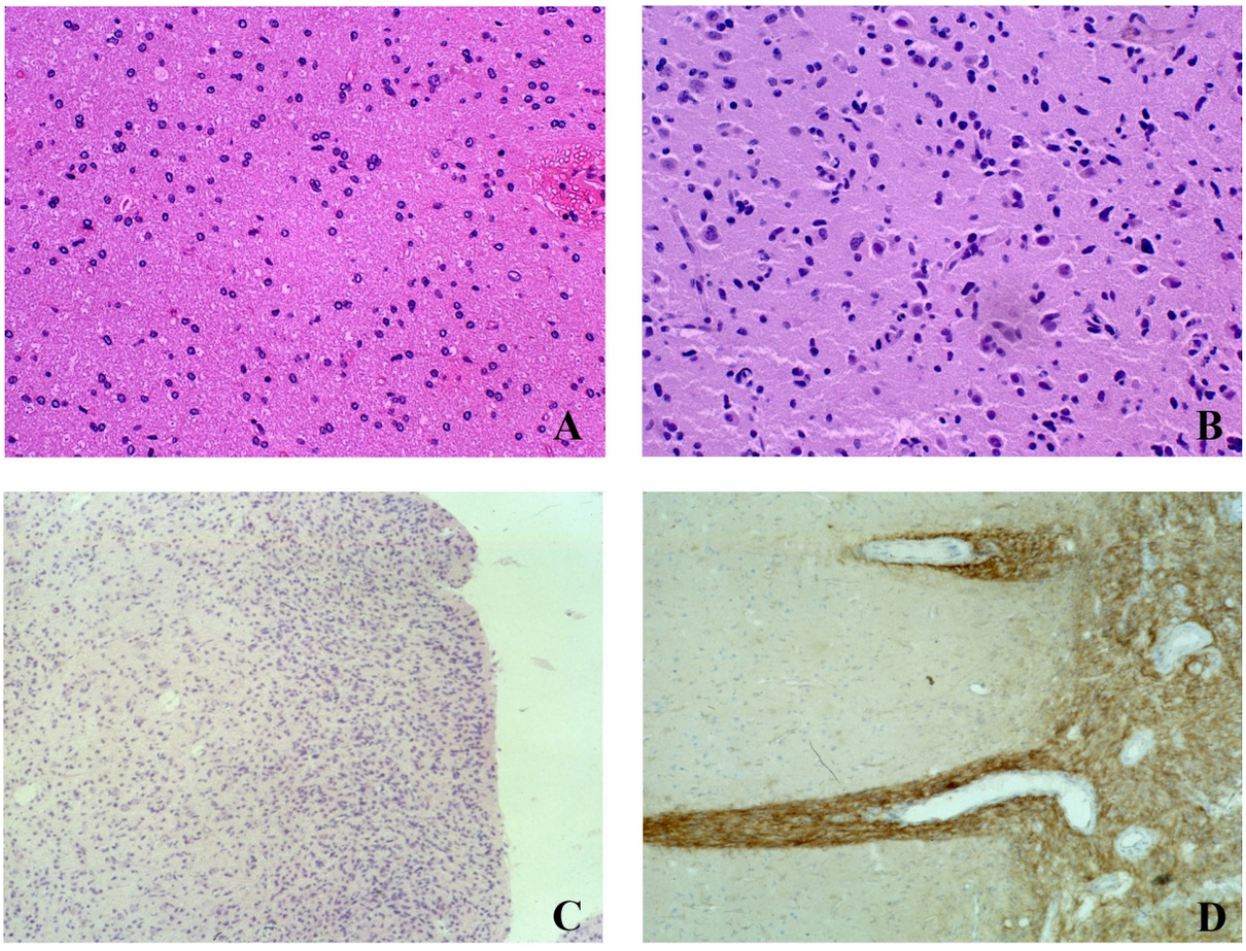

Figure 11. A – Mild infiltration. H&E, 200x; B – Strong infiltration. H&E, 200x; C – Sub-pial infiltration and growth. H&E, 100x; D – Infiltration along penetrating vessels from a tumor seeding in sub-arachnoidal space. PCNA, DAB, 100x.

may be included in the advancing tumor in which they progressively become no more recognizable from tumor cells. The question is whether they disappear suffocated by the high density of tumor cells or if they remain, unrecognizable from tumor cells, contributing to the pleomorphic aspect of gliomas, or if they are transformed into tumor cells [85].

Practically, two important points are that the tumor extends beyond the area of enhancement and that tumor cells can be found in peritumor edema [86]. In 20% of stereotactic biopsies tumor cells have been found in normal areas [87]. With the MRI era, detection of tumor infiltrating cells did not improve and it was shown that they can occur either in the T2-hyperintense areas or beyond them [88] or even in areas apparently normal in T1 or edematous in T2.

GBM spreads frequently along white matter tracts and their disruption can be detected by DTI. Observations have been made, but without any histological control. For example, infiltrated white matter shows a decrease of FA and an increase of ADC as when it is edematous. Displacement of white matter tracts with decreased FA can be recognized [89]. Many studies have been dedicated to FA reduction, but it did not appear to be sensitive enough to detect

infiltration [90]. The problem has not yet been resolved and it is still under discussion, because new techniques have been proposed [91,92], even though ADC values, lower in the tumor than in peritumor tissue, were not interpreted by others as significant [93]. Nevertheless, DTI is going to be accepted in the evaluation of tumor margins and invasiveness [94].

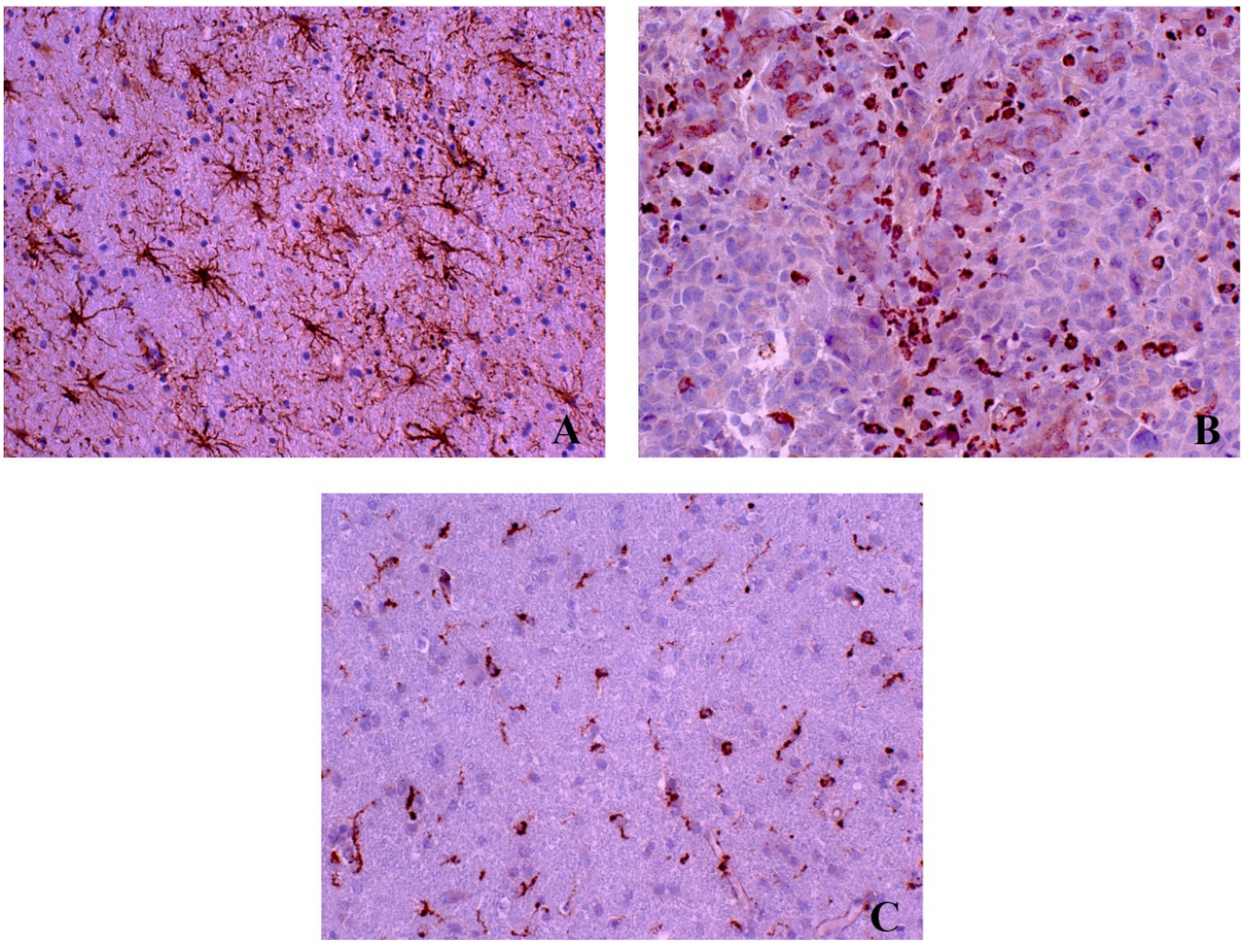

Figure 12. A – Reactive astrocytes at regular inter-distance. GFAP; B – Macrophages/microglia in the tumor. CD68; C – *id.* in peritumor area. CD68. All DAB, 200x.

Edema on T2-weighted imaging may have a high Cho/NAA ratio as in tumors [95] and this would indicate the occurrence of tumor cell infiltration [96] (Figure 13). It can be demonstrated by Aquaporin-4 antibody method (Figure 14A), but in the tissue this is not suitable for quantitative assessments. However, the real problem is how to detect mild infiltration, either alone or with edema. Some observations were supported by histological examination of peritumor edematous areas with or without cell infiltration. Three spectral patterns in peri-enhancing apparently edematous ROIs have been described: high Cho and abnormal Cho/NAA ratio in presumed tumor areas, normal Cho/NAA ratio in presumed edematous areas and Cho levels similar to normal, but with abnormal Cho/NAA ratio in tumor edema. In ROIs on peri-enhancing normal tissue, the patterns therefore could be: presumed infiltration with high Cho and abnormal Cho/NAA ratio and presumed normality with normal values.

http://dx.doi.org/10.5772/58391

These findings are in agreement with those indicating that tumor cells could be detected beyond the margin of the tumor by MRSI [97] and this has been substantiated by histopathology studies [88,96].

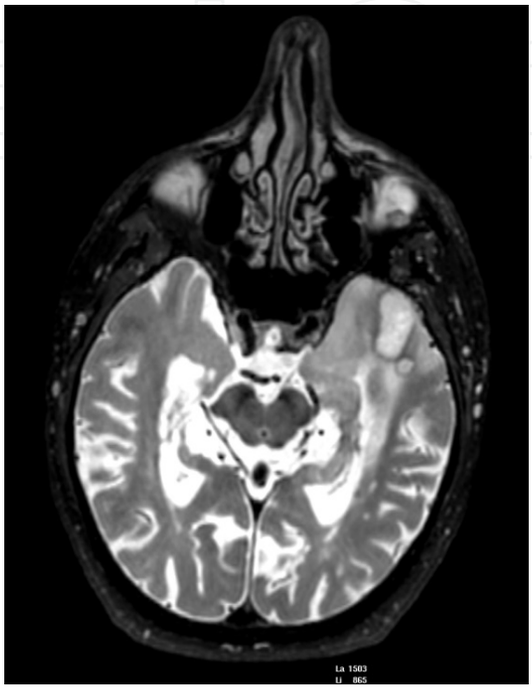

Figure 13. Axial contrast enhanced T1-weighted image, T2-weighted image, ADC and rCBV maps showing a lesion in the left frontal lobe with heterogeneous signal and diffusion properties, peripheral and irregular contrast enhancement. Perfusion is increased in the peripheral portion of the lesion.

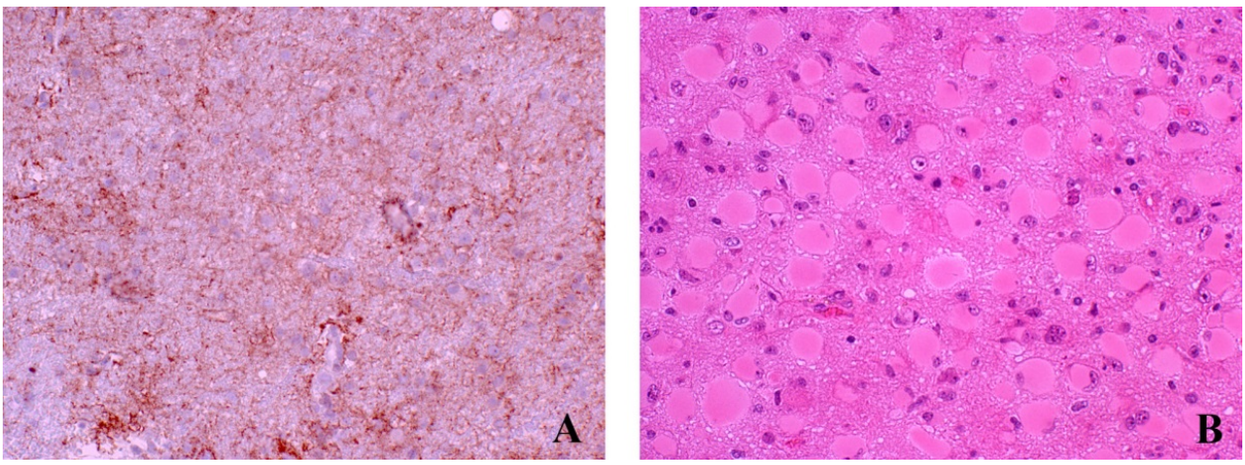

Figure 14. A – Aquaporin-4 in a peritumor area with astrocyte and vessel positive staining. DAB, 200x; B – Aspect of a gemistocytic astrocytoma found in a T2 hyper-intense area. H&E, 200x.

The overlapping of tumor cell infiltration and edema remains a major problem in the brain adjacent to tumor (BAT), because of the difficulty of their distinction [98,99], even though somebody supports that white matter fibre tract infiltration can be recognized [97]. In experimental tumors transplanted into mice, it has been observed by superimposing immunohistochemistry to MRI that in edema districts around the tumor, reactive astrocytes and activated microglia increased Aquaporin-4 expression and invasive tumor cells coexist [100]. Aquaporin-4 has been observed to correlate in peritumor tissue with edema and in the tumor with Hypoxia-Inducible Factor-1 (HIF-1), Vascular Endothelial Growth Factor (VEGF) and the grade of malignancy [101], whereas NAA seemed to be more suitable to detect low tumor infiltration in peritumor edema [102]. Of course, in the latter a damage to myelin sheaths takes place and it is detectable by MRSI [103].

In the recognition of tumor cell infiltration in edematous areas by MRI, histological examination of the surgical samples corresponding to the ROIs on rFSE or rFLAIR areas, is of great importance, in spite of the demonstration that removing T2 hyperintense non-enhancing areas and areas possibly containing ITCs, survival did not change [65]. It must be known that a T2 hyper-intense area may well correspond to a tumor (Figure 14B). A distinction would be possible, provided that there is no mismatch between the ROIs and sample removal. Usually, the cells composing edematous areas can be: tumor, normal or endothelial cells, macrophages or inflammatory cells and mainly reactive astrocytes. In our experience, the cell count is of paramount importance, especially when the number of non-tumor cells largely exceeds that of tumor cells, including in the former reactive astrocytes, microglia and endothelial cells. By comparing the number of cells in H&E stained sections and of GFAP+and CD68+cells with MRI variables, it has been found that normal cells, reactive astrocytes and microglia cells represent a rather stable quota of cells, so that variations of the total number of cells of a given area could be attributed to tumor cells. Reactive astrocytes, once no more proliferating, become fibrillogenetic and mature; usually, they do not exceed a certain number *per* field (Figure 12A). Therefore, they may influence the total number of cells only when tumor cell infiltration is mild. When the number of infiltrating cells is high, the astrocytic quota becomes insignificant. The same can be said for microglia/macrophages. Inside the tumor these cells are often found in perivascular or perinecrotic masses, but in peritumor tissue they are more regularly distributed and they too do not exceed a certain number *per* field (Figure 12B,C). CBV or Cho/NAA values will be influenced by macrophages/microglia only when the total number of cells is very low, *i.e.* when tumor cell infiltration will be really mild, below a certain percentage of the total number of cells, taking into account that the number of reactive astrocytes plus that of microglia/macrophages usually corresponds to the half of that of normal cells (unpublished data).

ITCs can be detected only after a systemic study of the brain at autopsy, as in the whole mounting preparation technique (Figure 15); they cannot be detected in surgical material because this usually cannot include them [4]. ITCs remain as a sword of Damocles in regard to tumor recurrence.

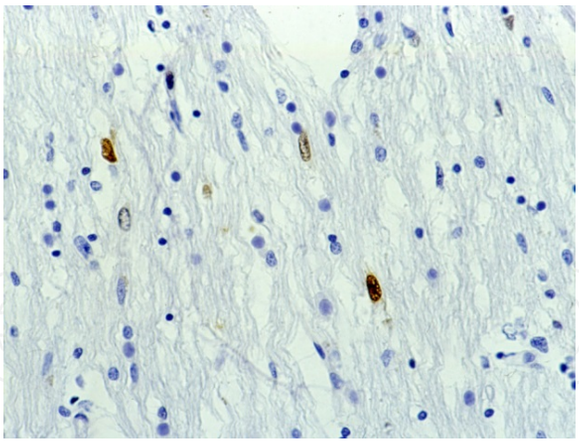

Figure 15. Isolate tumor cells in a white matter bundle. PCNA, DAB, 400x.

5. GSCs in the tumor: Target of therapies?

In the last decades, the aphorism is that the eradication of the tumor cannot be obtained by directing chemo-and radiotherapies to the entire tumor mass, composed of non-proliferating, differentiated and insensitive cells; on the contrary, such therapies would be successful if addressed to the cells responsible for growth, recurrence and resistance, *i.e.* GSCs. Therefore, the question is whether these cells can be *in vivo* detected by neuro-imaging and where are they located or generated in the tumor. To answer this question, a short discussion on the origin and nature of GSCs is necessary.

The hypothesis of GSCs is based on the concept that a rare subset of cells within GBM may have significant expansion capacity and the ability to generate new tumors. The remainder of tumor cells, which predominantly make up GBM, may represent partially differentiated cells with limited progenitor capacity or terminally differentiated cells that cannot form new tumors. Following the model of glioma origin from sub-ventricular zone (SVZ) after nitro-sourea derivatives [104], the most important hypothesis on gliomagenesis is today that GSCs derive by the transformation of Normal Stem Cells (NSCs) or progenitors, *i.e.* from B or C cells of the SVZ niche [105]. There is a great similarity between SVZ NSCs or progenitors and TICs and malignant gliomas most probably originate from the SVZ [106,107]. The concept is supported by the observation that GBM is almost always in contact with lateral ventricles [108]. This hypothesis cannot be applied to benign gliomas that should derive from mature glia. According to other hypotheses, also GBMs could derive from mature glial cells by acquiring stemness properties through a dedifferentiation process [109] or from stem cells of the white matter, NG2 cells. This origin would fit better with tumors far from the ventricles or with secondary GBM [110]. Also reactive astrocytes can be candidate for glioma origin [111,112], considering that they can acquire a stem-like phenotype [113].

GSCs develop in niches that can be perivascular or perinecrotic [114]. In perivascular niches there is a close contact between endothelial cells and Nestin+and CD133+cells [115]; the former would favor the self-renewal of the latter, mainly by Notch, and the opposite would happen

for angiogenesis through VEGF and hypoxia/HIF-1 [115-120]. In perinecrotic niches, GSCs are generated by hypoxia through HIF-1. Really, in the niches there can be a complicated relationship among different cell types, such as macrophages, pericytes, astrocytes, *etc.* with a multiple signalling [54,121,122]. In our experience, perinecrotic GSCs could be the remnants of GSCs that populated hyper-proliferating areas before the development of circumscribed necroses within them; this would take place because of the imbalance between the high proliferation capacity of tumor cells and the low one of endothelial cells [2,123]. GSCs, either as NS or AC, are heterogeneous as for stemness properties, clonogenicity and tumorigenicity and they have been regarded as at the top of a cell hierarchy for some molecular signs [49,50]. Stemness among tumor cells could be distributed in a spectrum with a *crescendo* from quiescent highly differentiated cells, where it is nil, to those in which it reaches the highest degree of expression. Stemness would be regulated by the microenvironment [53] and it could be the feature of a functional status rather than of a subset of cells [124,125]. As it is lost during differentiation of normal cytogenesis beyond the stage of progenitors, in the opposite way it is gained by dedifferentiating tumor cells when they reach the stage of progenitors.

The heterogeneity of GBM, before discussed, conditions different genetic assets of the cells in the different clones; going from the samples of the most malignant areas of the tumor to those of tumor periphery, the potential of generating NS or AC decreases. The conclusion is that stem cells are kept as such by microenvironments and these are realized in the most malignant sites of the tumor [51,55].

6. Location of GSCs in the tumor and their detection by neuro-imaging

If GSCs were considered as a subset of special cells, they should be located somewhere in the tumor and therefore their search *in vivo* could be justified. According to the hypothesis that they represent a functional status, they should appear in the tumor when and where, as the consequence of the transformation process, tumor cells reach the threshold of stemness. In some experience, NS would be generated from whatever part of GBM [126], whereas in some other experiences [48], different subsets of GSCs arise from regions of GBM with different malignancy potential, showing different tumorigenic potential and genetic abnormalities, even though originating from the same ancestor cell. Since GSCs reside in niches, their distribution in the tumor should follow that of niches which in turn with their microenvironments develop where malignancy occurs [52]. On the other hand, it has been observed that GSCs occur in the hypoxic area between the central necrosis and the proliferating zone of GBM [127].

Until today, the only mean to detect GSCs is to apply the neurosphere assay to the surgical samples removed from different parts of the tumor. Their recognition can be therefore achieved only after surgery. It would be highly useful to know in advance where in tumor GSCs are located or generated in order to try to annihilate them without surgery and to cure the patient. Can they be detected by MRI or other procedures *in vivo*?

Animal *in vivo* imaging techniques have been applied to some stem cell populations – hematopoietic and leukemic stem cells – but the application to solid tissues has been limited [41].

http://dx.doi.org/10.5772/58391

Using intravital microscopy, labelled GSCs could be followed in their propagation and responsibility in producing glioma heterogeneity [41], but data are not available by MRI techniques. Bone marrow-derived endothelial precursors, labelled by super-paramagnetic iron oxide nanoparticles, could be demonstrated in glioma-bearing immunodeficient SCID mice by MRI [128], but no similar procedure has been adopted for GSCs. The only possibility is to use the spatial relationship between MRI variables and tumor phenotypes [33] including into the phenotype the expression of GSC stemness status.

Acknowledgements

This work was supported by Grant n. 4011 SD/cv 2011-0438 from Compagnia di San Paolo, Turin, Italy.

Author details

Davide Schiffer[1], Consuelo Valentini[2], Antonio Melcarne[3], Marta Mellai[1], Elena Prodi[2], Giovanna Carrara[2], Tetyana Denysenko[1,3], Carola Junemann[3], Cristina Casalone[4], Cristiano Corona[4], Valentina Caldera[1], Laura Annovazzi[1], Angela Piazzi[1], Paola Cassoni[5], Rebecca Senetta[5], Piercarlo Fania[6] and Angelina Cistaro[6,7]

1 Neuro-bio-oncology Center of Policlinico di Monza Foundation, Vercelli, Italy

2 Neuroradiology Unit, CTO Hospital, Turin, Italy

3 Neurosurgery Unit, CTO Hospital, Turin, Italy

4 Istituto Zooprofilattico, Turin, Italy

5 Department Medical Sciences, University of Turin, Turin, Italy

6 Positron Emission Tomography Center IRMET S.p.A, Euromedic inc., Turin, Italy

7 Institute of Cognitive Sciences and Technologies, National Research Council, Rome, Italy

References

[1] Coons SW, Johnson PC, Scheithauer BW, Ytes AJ, Pearl DK. Improving diagnostic accuracy and interobserver concordance in the classification and grading of primary gliomas. Cancer 1997; 79(7): 1381-1393.

[2] Schiffer D, Chiò A, Giordana MT, Mauro A, Migheli A, et al. The vascular response to tumor infiltration in malignant gliomas. Morphometric and reconstruction study. Acta Neuropathologica 1989; 77(4): 369-378.

[3] Schiffer D. Brain tumors: biology, pathology and clinical references. Berlin, Heidelberg, New York: Springer; 1997.

[4] Schiffer D. Brain tumor pathology. Current diagnostic hotspots and pitfalls. Dordrecht: Springer; 2006.

[5] Alavi JB, Alavi A, Chawluk J, Kushner M, Powe J, et al. Positron emission tomography in patients with glioma. A predictor of prognosis. Cancer 1988; 62(6): 1074-1078.

[6] Padma MV, Said S, Jacobs M, Hwang DR, Dunigan K, et al. Prediction of pathology and survival by FDG PET in gliomas. Journal of Neuro-Oncology 2003: 64(3): 227-237.

[7] Kitis O, Altay H, Calli C, Yunten N, Akalin T, et al. Minimum apparent diffusion coefficients in the evaluation of brain tumors. European Journal of Radiology 2005; 55(3): 393-400.

[8] Murakami R, Hirai T, Sugahara T, Fukuoka H, Toya R, at al. Grading astrocytic tumors by using apparent diffusion coefficient parameters: superiority of a one-versus two-parameter pilot method. Radiology 2009; 251(3): 838-845.

[9] Kang Y, Choi SH, Kim YJ, Kim KG, Sohn CH, et al. Gliomas: histogram analysis of apparent diffusion coefficient maps with standard-or high-b-value diffusion-weighted MR imaging-correlation with tumor grade. Radiology 2011; 261(3): 882-890.

[10] Castillo M, Smith JK, Kwock L, Wilber K. Apparent diffusion coefficients in the evaluation of high-grade cerebral gliomas. AJNR American Journal of Neuroradiology 2001; 22(1): 60-64.

[11] Cha S. Update on brain tumor imaging: from anatomy to physiology. American Journal of Neuroradiology 2006; 27(3): 475-487.

[12] Law M, Cha S, Knopp EA, Johnson G, Arnett J, et al. High-grade gliomas and solitary metastases: differentiation by using perfusion and proton spectroscopic MR imaging. Radiology 2002; 222(3): 715-721.

[13] Yang S, Zhang C, Zhu T, Cai L, Gao S, et al. Resection of gliomas using positron emission tomography/computer tomography neuronavigation. Neurologia Medico-Chirurgica (Tokyo) 2007; 47(9): 397-401.

[14] Howe FA, Barton SJ, Cudlip SA, Stubbs M, Saunders DE, et al. Metabolic profiles of human brain tumors using quantitative in vivo 1H magnetic resonance spectroscopy. Magnetic Resonance in Medicine 2003; 49(2): 223-232.

[15] Al-Okaili RN, Krejza J, Wang S, Woo JH, Melhem ER. Advanced MR imaging techniques in the diagnosis of intraaxial brain tumors in adults. Radiographics 2006; 26(Suppl 1): S173-189.

[16] Jellison BJ, Field AS, Medow J, Lazar M, Salamat MS, et al. Diffusion tensor imaging of cerebral white matter: a pictorial review of physics, fiber tract anatomy, and tumor imaging patterns. American Journal of Neuroradiology 2004; 25(3): 356-369.

[17] Lu S, Ahn D, Johnson G, Law M, Zagzag D, et al. Diffusion-tensor MR imaging of intracranial neoplasia and associated peritumoral edema: introduction of the tumor infiltration index. Radiology 2004; 232(1): 221-228.

[18] White ML, Zhang Y, Yub F, Jaffar Kazmi SA. Diffusion tensor MR imaging of cerebral gliomas: evaluating fractional anisotropy characteristics. American Journal of Neuroradiology 2011; 32(2): 374-381.

[19] Shuyuan Y, Chuan Z, Shuyuan Y, Li C, Shuo G, et al. Preoperative estimation and resection of gliomas using positron emission tomography/computed tomography neuronavigation. In: Garami M. (ed.) Management of CNS tumors. Rijeka: InTech; 2012. p179-196.

[20] Jacobs AH, Kracht LW, Gossmann A, Rüger MA, Thomas AV, et al. Imaging in neurooncology. The Journal of the American Society of Experimental NeuroTherapeutics 2005; 2(2): 333-347.

[21] Di Chiro G, DeLaPaz RL, Brooks RA, Sokoloff L, Kornblith PL, et al. Glucose utilization of cerebral gliomas measured by [18F] fluorodeoxyglucose and positron emission tomography. Neurology 1982; 32(12): 1323-1329.

[22] Delbeke D, Meyerowitz C, Lapidus RL, Maciunas RJ, Jennings MT, et al. Optimal cutoff levels of F-18 fluorodeoxyglucose uptake in the differentiation of low-grade from high-grade brain tumors with PET. Radiology 1995; 195(1): 47-52.

[23] Stanescu L, Ishak GE, Khanna PC, Biyyam DR, Shaw DW, et al. FDG PET of the brain in pediatric patients: imaging spectrum with MR imaging correlation. Radiographics 2013; 33(5): 1279-1303.

[24] Bénard F, Romsa J, Hustinx R. Imaging gliomas with positron emission tomography and single-photon emission computed tomography. Seminars in Nuclear Medicine 2003; 33(2): 148-162.

[25] Chen W. Clinical applications of PET in brain tumors. Journal of Nuclear Medicine 2007; 48(9): 1468-1481.

[26] Kato T, Shinoda J, Oka N, Miwa K, Nakayama N, et al. Analysis of 11C-methionine uptake on low-grade gliomas and correlation with proliferative activity. American Journal of Neuroradiology 2008; 29(10): 1867-1871.

[27] Cistaro A. Atlas of PET/CT in pediatric patients. Dordrecht: Springer; 2013.

[28] Stadlbauer A, Prante O, Nimsky C, Salomonowitz E, Buchfelder M, et al. Metabolic imaging of cerebral gliomas: spatial correlation of changes in O-(2-18F-fluoroethyl)-L-tyrosine PET and proton magnetic resonance spectroscopic imaging. Journal of Nuclear Medicine 2008; 49(5): 721-729.

[29] Airley RE, Monaghan JE, Jane N. Hypoxia and disease: opportunities for novel diagnostic and therapeutic prodrug strategies. Pharmaceutical Journal 2000; 264(7094): 666-673.

[30] Bernsen HJ, Rijken PF, Peters H, Raleigh JA, Jeuken JW, et al. Hypoxia in a human intracerebral glioma model. Journal of Neurosurgery 2000; 93(3): 449-454.

[31] Bruehlmeier M, Roelcke U, Schubiger PA, Ametamey SM. Assessment of hypoxia and perfusion in human brain tumors using PET with 18F-fluoromisonidazole and 15O-H2O. Journal of Nuclear Medicine 2004; 45(11): 1851-1859.

[32] Barajas RF Jr, Hodgson JG, Chang JS, Vandenberg SR, Yeh RF, et al. Glioblastoma multiforme regional genetic and cellular expression patterns: influence on anatomic and physiologic MR imaging. Radiology 2010; 254(2): 564-576.

[33] Barajas RF Jr, Phillips JJ, Parvataneni R, Molinaro A, Essock-Burns E, et al. Regional variation in histopathologic features of tumor specimens from treatment-naive glioblastoma correlates with anatomic and physiologic MR Imaging. Journal of Neuro-Oncology 2012; 14(7): 942-954.

[34] Di Costanzo A, Scarabino T, Troisi F, Popolizio T, Catapano D, et al. Proton MR spectroscopy of cerebral gliomas at 3 T: spatial heterogeneity, and tumour grade and extent. European Radiology 2008; 18(8): 1727-1735.

[35] Miwa K, Shinoda J, Yano H, Okumura A, Iwama T, et al. Discrepancy between lesion distribution on methionine PET and MR images in patients with glioblastoma multiforme: insight from a PET and MR fusion image study. Journal of Neurology, Neurosurgery and Psychiatry 2004; 75(10): 1457-1462.

[36] Jacobs AH, Thomas A, Kracht LW, Li H, Dittmar C, et al. 18F-fluoro-L-thymidine and 11C-methylmethionine as markers of increased transport and proliferation in brain tumors. Journal of Nuclear Medicine 2005; 46(12): 1948-1958.

[37] Chen W, Cloughesy T, Kamdar N, Satyamurthy N, Bergsneider M, et al. Imaging proliferation in brain tumors with 18F-FELT PET: comparison with 18F-FDG. Journal of Nuclear Medicine 2005; 46(6): 945-952.

[38] Price SJ, Fryer TD, Cleij MC, Dean AF, Joseph J, et al. Imaging regional variation of cellular proliferation in gliomas using 3′-deoxy-3′-[18F]fluorothymidine positron emission tomography: an image-guided biopsy study. Clinical Radiology 2008; 64(1): 52-63.

[39] Stadlbauer A, Pölking E, Prante O, Nimsky C, Buchfelder M, et al. Detection of tumour invasion into the pyramidal tract in glioma patients with sensorimotor deficits

by correlation of (18)F-fluoroethyl-L-tyrosine PET and magnetic resonance diffusion tensor imaging. Acta Neurochirurgica (Wien) 2009; 151(9): 1061-1069.

[40] Giese A, Loo MA, Tran N, Haskett D, Coons SW, et al. Dichotomy of astrocytoma migration and proliferation. International Journal of Cancer 1996; 67(2): 275-282.

[41] Lathia JD, Gallagher J, Myers JT, Li M, Vasanji A, et al. Direct in vivo evidence for tumor propagation by glioblastoma cancer stem cells. Public Library of Science One 2011; 6(9): e24807.

[42] Mazzoleni S, Galli R. Gliomagenesis: a game played by few players or a team effects? Frontiers in Neuroscience 2012; 4(1): 205-213.

[43] Reya T, Morrison SJ, Clarke MF, Weissman IL. Stem cells, cancer, and cancer stem cells. Nature 2001; 414(6859): 105-108.

[44] Adams JM, Strasser A. Is tumor growth sustained by rare cancer stem cells or dominant clones? Cancer Res 2008; 68(11): 4018-4021.

[45] de Almeida Sassi F, Lunardi Brunetto A, Schwartsmann G, Roesler R, Abujamra AL. Glioma revisited: from neurogenesis and cancer stem cells to the epigenetic regulation of the niche. Journal of Oncology 2012; 2012: 537861.

[46] Sun Y, Goderie SK, Temple S. Asymmetric distribution of EGFR receptor during mitosis generates diverse CNS progenitor cells. Neuron 2005; 45(6): 873-886.

[47] De Bacco F, Casanova E, Medico E, Pellegatta S, Orzan F, et al. The MET oncogene is a functional marker of a glioblastoma stem cell subtype. Cancer Research 2012; 72(17): 4537-4550.

[48] Piccirillo SG, Combi R, Cajola L, Patrizi A, Redaelli S, et al. Distinct pools of cancer stem-like cells coexist within human glioblastomas and display different tumorigenicity and independent genomic evolution. Oncogene 2009; 28(15): 1807-1811.

[49] Chen R, Nishimura MC, Bumbaca SM, Kharbanda S, Forrest WF, et al. A hierarchy of self-renewing tumor-initiating cell types in glioblastoma. Cancer Cell 2010; 17(4): 362-375.

[50] Mazzoleni S, Politi LS, Pala, M. Cominelli M, Franzin A, et al. Epidermal growth factor receptor expression identifies functionally and molecularly distinct tumor-initiating cells in human glioblastoma multiforme and is required for gliomagenesis. Cancer Research 2010; 70(19): 7500-7513.

[51] Caldera V, Mellai M, Annovazzi L, Piazzi A, Lanotte M, et al. Antigenic and genotypic similarity between primary glioblastomas and their derived neurospheres. Journal of Oncology 2011; 2011: 314962.

[52] Schiffer D, Mellai M, Annovazzi L, Piazzi A, Monzeglio O, et al. Glioblastoma cancer stem cells: basis for a functional hypothesis. Stem Cell Discovery 2012; 2(3): 122-131.

[53] Charles NA, Holland EC, Gilbertson R, Glass R, Kettenmann H. The brain tumor microenvironment. Glia 2012; 60(3): 502-514.

[54] Filatova A, Acker T, Garvalov BK. The cancer stem cell niche(s): the crosstalk between glioma stem cells and their microenvironment. Biochimica et Biophysica Acta 2013; 1830(2): 2496-2508.

[55] Schiffer D, Mellai M, Annovazzi L, Caldera V, Piazzi A, et al. Stem cell niches in glioblastoma. A neuropathological view. Submitted.

[56] Dunn KW, Kamocka MM, McDonald JH. A practical guide to evaluating colocalization in biological microscopy. American Journal of Physiology. Cell Physiology 2011; 300(4): C723-742.

[57] Adler J, Parmryd I. Quantifying colocalization by correlation: the Pearson correlation coefficient is superior to the Mander's overlap coefficient. Cytometry 2010; 77(8): 733-742.

[58] Górska-Chrzastek M, Grzelak P, Bieńkiewicz M, Tybor K, Zakrzewska E, et al. Assessment of clinical usefulness of 131I alpha-methyl-tyrosine and fused SPECT/MRI imaging for diagnostics of recurrent cerebral gliomas. Nuclear Medicine Review. Central & Eastern Europe 2004; 7(2): 135-141.

[59] Burger PC, Heinz ER, Shibata T, Kleihues P. Topographic anatomy and CT correlations in untreated glioblastoma multiforme. Journal of Neurosurgery 1988; 68(5): 698-704.

[60] Shapiro WE. Current therapy for brain tumors: back to the future. Archives of Neurology 1999; 56(4): 429-432.

[61] Schiffer D, Annovazzi L, Caldera V, Mellai M. The brain adjacent to tumor (BAT). In: Garami M. (ed.) Management of CNS tumors. Rijeka, InTech; 2011. p197-224.

[62] Caffo M, Barresi V, Caruso G, La Fata G, Pino MA, et al. Gliomas biology: angiogenesis and invasion. In: Lichtor T. (ed.) Evolution of the molecular biology of brain tumors and the therapeutic implications. Rijeka, InTech; 2013. p37-103.

[63] Province P, Griguer CE, Han X, Louis NB, Shaykh HF. Hypoxia, angiogenesis and mechanisms for invasion of malignant gliomas. In: Lichtor T. (ed.) Evolution of the molecular biology of brain tumors and the therapeutic implications. Rijeka, InTech; 2013. p105-123.

[64] Mangiola A, de Bonis P, Maira G, Balducci M, Sica G, et al. Invasive tumor cells and prognosis in a selected population of patients with glioblastoma multiforme. Cancer 2008; 113(4): 841-846.

[65] Ramakrishna R, Barber J, Kennedy G, Rizvi A, Goodkin R, et al. Imaging features of invasion and preoperative and postoperative tumor burden in previously untreated

glioblastoma: correlation with survival. Surgical Neurology International 2010; 1(1): 40-51.

[66] Glas M, Rath BH, Simon M, Reinartz R, Schramme A, et al. Residual tumor cells are unique cellular targets in glioblastoma. Annals of Neurology 2010; 68(2): 264-269.

[67] Kitai R, Horita R, Sato K, Yoshida K, Arishima H, et al. Nestin expression in astrocytic tumors delineates tumor infiltration. Brain Tumor Pathology 2010; 27(1): 17-21.

[68] Capper D, Weissert S, Balss J, Habel A, Meyer J, et al. Characterization of R132H mutation-specific IDH1 antibody binding in brain tumors. Brain Pathology 2010; 20(1): 245-254.

[69] Schiffer D. Neuropathology and imaging: the ways in which gliomas spreads and varies in its histological aspects, In: Walker and DGT Thomas (ed.) Biology of brain tumors. Boston, Nijhoff: 1986. p286-290.

[70] Nishio S, Korosue K, Tateishi J, Fukui M, Kitamura K. Ventricular and subarachnoid seeding of intracranial tumors of neuroectodermal origin-a study of 26 consecutive autopsy cases with reference to focal ependymal defect. Clinical Neuropathology 1982; 1(2): 83-91.

[71] Rosenblum ML. Factors influencing tumor cell traffic in the central nervous system. Surgical Neurology 1995; 43(6): 595.

[72] Pilkington GJ. Glioma heterogeneity in vitro: the significance of growth factor and gangliosides. Neuropathology and Applied Neurobiology 1992; 18(5): 434-432.

[73] Merzak A, Koochekpour S, Dkhissi F, Raynal S, Lawrence D, et al. Synergism between growth-factors in the control of glioma cell-proliferation, migration and invasion in-vitro. International Journal of Oncology 1995; 6(5): 1079-1085.

[74] Dalrymple SJ, Parisi JE, Roche PC, Ziesmer SC, Scheithauer BW, et al. Changes in proliferating cell nuclear antigen expression in glioblastoma multiforme cells along a stereotactic biopsy trajectory. Neurosurgery 1994; 35(6): 1036-1044.

[75] Roggendorf W, Strupp S, Paulus W. Distribution and characterization of microglia/macrophages in human brain tumors. Acta Neuropathologica 1996; 92(3): 288-293.

[76] Morimura T, Neuchrist C, Kitz K, Budka H, Scheiner O, et al. Monocyte subpopulations in human gliomas: expression of Fc and complement receptors and correlation with tumor proliferation. Acta Neuropathologica 1990; 80(3): 287-294.

[77] Yi L, Xiao H, Xu M, Ye X, Hu J, et al. Glioma-initiating cells: A predominant role in microglia/macrophages tropism to glioma. Journal of Neuroimmunology 2011; 232(1-2): 75-82.

[78] Graeber MB, Scheithauer BW, Kreutzberg GW. Microglia in brain tumors. Glia 2002; 40(2): 252-259.

[79] Zhai H, Heppner FL, Tsirka SE. Microglia/macrophages promote glioma progression. Glia 2011; 59(3): 472-485.

[80] Bushong EA, Martone ME, Ellisman MH. Maturation of astrocyte morphology and the establishment of astrocyte domains during postnatal hippocampal development. International Journal of Developmental Neuroscience 2004; 22(2): 73-86.

[81] Clarke SR, Shetty AK, Bradley JL, Turner DA. Reactive astrocytes express the embryonic intermediate neurofilament nestin. Neuroreport 1994; 5(15): 1885-1888.

[82] Eliasson C, Sahlgren C, Berthold CH, Stakeberg J, Celis JE, et al. Intermediate filament protein partnership in astrocytes. The Journal Biological Chemistry 1999; 274(34): 23996-24006.

[83] Mandonnet E, Capelle L, Duffau H. Extension of paralimbic low grade gliomas: toward an anatomical classification based on white matter invasion patterns. Journal of Neuro-Oncology 2006; 78(2): 179-185.

[84] Ellingson BM, LaViolette PS, Rand SD, Malkin MG, Connelly JM, Mueller, et al. Spatially quantifying microscopic tumor invasion and proliferation using a voxel-wise solution to a glioma growth model and serial diffusion MRI. Magnetic Resonance in Medicine 2011; 65(4): 1131-1143.

[85] Tamagno I, Schiffer D. Nestin expression in reactive astrocytes of human pathology. J Neuro-Oncology 2006; 80(3): 227-233.

[86] Selker RG, Mendelow H, Walker M, Sheptak PE, Phillips JG. Pathological correlation of CT ring in recurrent previously treated gliomas. Surgical Neurology 1982; 17(4): 251-254.

[87] Kelly PJ, Daumas-Duport C, Kispert DB, Kall BA, Scheithauer BW, et al. Imaging-based stereotaxic serial biopsies in untreated intracranial glial neoplasms. Journal of Neurosurgery 1987; 66(6): 865-874.

[88] Watanabe M, Tanaka R, Takeda N. Magnetic resonance imaging and histopathology of cerebral gliomas. Neuroradiology 1992; 34(6): 463-469.

[89] Witwer BP, Moftakhar R, Hasan KM, Deshmukh P, Haughton V, et al. Diffusion-tensor imaging of white matter tracts in patients with cerebral neoplasm. Journal of Neurosurgery 2002; 97(3): 568-575.

[90] Price SJ, Gillard JH. Imaging biomarkers of brain tumour margin and tumour invasion. The British Journal of Radiology 2011; 84(Spec No 2): S159-167.

[91] Zhou XJ, Leeds NE, Poonawalla AH, Weinberg J. Assessment of tumor cell infiltration along white matter fiber using diffusion tensor imaging. Proceedings of the International Society for Magnetic Resonance in Medicine 2003; 11: 2238.

[92] Price SJ, Peña A, Burnet NG, Pickard JD, Gillard JH. Detecting glioma invasion of the corpus callosum using diffusion tensor imaging. The British Journal of Neurosurgery 2004; 18(4): 391-395.

[93] Pauleit D, Langen KJ, Floeth F, Hautzel H, Riemenschneider MJ, et al. Can the apparent diffusion coefficient be used as a non invasive parameter to distinguish tumor tissue from peritumoral tissue in cerebral gliomas? Journal of Magnetic Resonance Imaging 2004; 20(5): 758-764.

[94] Price SJ, Jena R, Burnet NG, Carpenter TA, Pickard JD, et al. Predicting patterns of glioma recurrence using diffusion tensor imaging. European Radiology 2007; 17(7): 1675-1684.

[95] McKnight TR, von dem Bussche MH, Vigneron DB, Lu Y, Berger MS, et al. Histopathological validation of three-dimensional magnetic resonance spectroscopy index as a prediction of tumor presence. Journal of Neurosurgery 2002; 97(4): 794-802.

[96] Croteau D, Scarpace L, Hearshen D, Gutierrez J, Fisher JL, et al. Correlation between magnetic resonance spectroscopy imaging and image-guided biopsies: semiquantitative and qualitative histopathological analyses of patients with untreated glioma. Neurosurgery 2001; 49(4): 823-829.

[97] Pirzkall A, Li X, Oh J, Chang S, Berger MS, et al. 3D MRSI fro resected high-grade gliomas before RT: tumor extent according to metabolic activity in relation to MRI. International Journal of Radiation Oncology, Biology, Physics 2004; 59(1): 126-137.

[98] Law M, Cha S, Knopp EA, Johnson G, Arnett J, et al. High-grade gliomas and solitary metastases: differentiation by using perfusion and proton spectroscopy MR imaging. Radiology 2002; 222(3): 715-722.

[99] Nelson SJ. Multivoxel magnetic resonance spectroscopy of brain tumors. Molecular Cancer Therapeutics 2003; 2(5): 497-507.

[100] Engelhorn T, Savaskan NE, Schwarz MA, Kreutzer J, Meyer EP, et al. Cellular characterization of the peritumoral edema zone in malignant brain tumors. Cancer Science 2009; 100(10): 1856-1862.

[101] Mou K, Chen M, Mao Q, Wang p, Ni R, et al. APQ-4 in peritumoral edematous tissue is correlated with the degree of glioma and with expression of VEGF and HIF-alpha. Journal of Neuro-Oncology 2010; 100(3): 375-383.

[102] Stadlbauer A, Nimsky C, Buslei R, Pinker K, Gruber S, et al. Proton magnetic resonance spectroscopic imaging in the borderzone of gliomas. Correlation of metabolic and histological changes at low tumor infiltration-initial results. Investigative Radiology 2007; 42(4): 218-223.

[103] Ricci R, Bacci A, Tugnoli V, Battaglia S, Maffei M, et al. Metabolic findings on 3T 1H-MR spectroscopy in peritumoral brain edema. AJNR American Journal of Neuroradiology 2007; 28(7): 1287-1291.

[104] Schiffer D, Annovazzi L, Caldera V, Mellai M. On the origin and growth of gliomas. Anticancer Research 2010; 30(6): 1977-1998.

[105] Holland EC. Progenitor cells and glioma formation. Current Opinion in Neurology 2001; 14(6): 683-688.

[106] Alcantara Llaguno S, Chen J, Kwon CH, Jackson EL, Li Y, et al. Malignant astrocytomas originate from neural stem/progenitor cells in a somatic tumor suppressor mouse model. Cancer Cell 2009; 15(1): 45-56.

[107] Jaques TS, Swales A, Brzozowski MJ, Henriquez MV, Linehan JN, et al. Combinations of genetic mutations in the adult neural stem cell compartment determine brain tumour phenotypes. The EMBO Journal 2010; 29(1): 222-235.

[108] Barami K, Sloan AE, Rojiani A, Schell MJ, Staller A, et al. Relationship of gliomas to the ventricular walls. Journal of Clinical Neuroscience 2009; 16(2): 195-201.

[109] Sanai N, Alvarez-Buylla, Berger MS. Neural stem cells and the origin of gliomas. The New England Journal of Medicine 2005; 353(8): 811-822.

[110] Siebzehnrubl FA, Reynolds BA, Vescovi A, Steindler DA, Deleyrolle LP. The origins of glioma: e pluribus unum? Glia 2011; 59(8): 1135-1147.

[111] Dufour C, Cadusseau J, Varlet P, Surena AL, de Faira GP, et al. Astrocytes reverted to a neural progenitor-like state with transforming growth factor alpha are sensitized to cancerous transformation. Stem Cells 2009; 27(10): 2373-2382.

[112] Silver DJ, Steindler DA. Common astrocytic programs during brain development, injury and cancer. Trends in Neurosciences 2009; 32(6): 303-311.

[113] Buffo A, Rite I, Tripathi P, Lepier A, Colak D, et al. Origin and progeny of reactive gliosis: a source of multipotent cells in the injured brain. Proceedings of the Natural Academy of Sciences USA 2008; 105(9): 3581-3586.

[114] Li L, Neaves WB. Normal stem cells and cancer stem cells: the niche matters. Cancer Research 2006; 66(9): 4553-4557.

[115] Calabrese C, Poppleton H, Kokac M, Hogg TL, Fuller C, et al. A perivascular niche for brain tumor stem cells. Cancer Cell 2007; 11(1): 69-82.

[116] Bao S, Wu S, Sathornsumetee S, Hao Y, Li Z, et al. Stem cell-like glioma cells promote tumor angiogenesis through vascular endothelial growth factor. Cancer Research 2006; 66(16): 7843-7848.

[117] Jensen RL, Ragel BT, Whang K, Gillespie D. Inhibition of hypoxia inducible factor-1 alpha (HIF-1 alpha) decreases vascular endothelial growth factor (VEGF) secretion and tumor growth in malignant gliomas. Journal of Neuro-Oncology 2006; 78(3): 233-247.

[118] Folkins C, Shaked Y, Man S, Tang T, Lee CR, et al. Glioma tumor stem-like cells promote tumor angiogenesis and vasculogenesis via vascular endothelial growth factor and stromal-derived factor 1. Cancer Research 2009; 69(18): 7243-7251.

[119] Bar EE, Lin A, Mahairaki V, Matsui W, Eberhart CG. Hypoxia increases the expression of stem-cell markers and promotes clonogenicity in glioblastoma neurospheres. The American Journal of Pathology 2010; 177(3): 1491-1502.

[120] Charles N, Holland EC. The perivascular niche microenvironment in brain tumor progression. Cell Cycle 2010; 9(15): 3012-3021.

[121] Christensen K, Schrøder HD, Kristensen BW. CD133 identifies perivascular niches in grade II-IV astrocytomas. Journal of Neuro-Oncology 2008; 90(2): 157-170.

[122] Seidel S, Garvalov BK, Wirta V, von Stechow L, Schänzer A, et al. A hypoxic niche regulates glioblastoma stem cells through hypoxia inducible factor 2 alpha. Brain 2010; 133(Pt4): 983-995.

[123] Kargiotis O, Rao JS, Kyritsis AP. Mechanisms of angiogenesis in gliomas. Journal of Neuro-Oncology 2006; 78(3): 281-293.

[124] Zipori D. The nature of stem cells: state rather than entity. Nature Review Genetics 2004; 5(11): 873-878.

[125] Reynolds BA, Vescovi AL. Brain cancer stem cells: think twice before going flat. Cell Stem Cell 2009; 5(5): 466-467.

[126] Pallini R, Ricci-Vitiani L, Banna GL, Signore M, Lombardi D, et al. Cancer stem cell analysis and clinical outcome in patients with glioblastoma multiforme. Clinical Cancer Research 2008; 14(24): 8205-8212.

[127] Persano L, Rampazzo E, Della Puppa A, Pistollato F, Basso G. The three-layer concentric model of glioblastoma: cancer stem cells, microenvironmental regulation, and therapeutic implications. TheScientificWorldJournal 2011; 11: 1829-1841.

[128] Anderson S, Glod J, Arbab AS, Noel M, Ashari P, et al. Noninvasive MR imaging of magnetically labelled stem cells in directly identify neovasculature in a glioma model. Blood 2005; 105(1): 420-425.

IntechOpen